

Electron Charge Distribution in Orbitrons

M. PORTO PATO

Departamento de Física Nuclear", Instituto de Física da Universidade de São Paulo, São Paulo SP

and

L. C. GOMES

*Centro Brasileiro de Pesquisas Físicas *, Conselho Nacional de Desenvolvimento Científico e Tecnológico (CNPq), Rio de Janeiro RJ*

Recebido em 14 de Junho de 1976

The theoretical assumptions that lead to the determination of the single electron phase space distribution functions in orbitrons are discussed. The models of Hooverman, Feaks et *al.* and Deichelbohrer are analyzed and compared with the model used by Oliveira, Pato and Rogério. The ion energy spectrum measurement of Cybulska and Douglas is interpreted on the basis of the model by Oliveira et *al.*.

As hipóteses teóricas que levam à determinação da função de distribuição no espaço das fases do elétron em órbitrons são discutidas. Os modelos de Hooverman, Feaks et *al.* e Deichelbohrer são analisados e comparados com o modelo usado por Oliveira, Pato e Rogério. A medida do espectro de energia de ions, de Cybulska e Douglas, é interpretada em base ao modelo de Oliveira et *al.*.

* Postal address: Caixa Postal 20516, 01000-São Paulo, SP.

** Postal address: Av. Wenceslau Braz, 72, 20000-Rio de Janeiro, RJ.

1. INTRODUCTION

Electrostatic electron containment was proposed, in 1963, by Herb, Pauly and Fisher¹ using a device consisting essentially of a cylindrical condenser, where the outer cylinder, the cathode, is grounded and the inner cylinder, the anode, is kept at a positive potential, commonly of the order of 10^3 V. Electrons are injected, in the region between the cylinders, by a filament geometrically arranged in such a way that an appreciable proportion of the electrons leave the injector region, with sufficient angular momentum to avoid hitting the anode. The filament is maintained at a positive bias for the electrons to be repelled by the cathode and end plates. This device was called an orbitron, and proposed both as an ionization gauge² and an ion vacuum pump³. The attractive feature of orbitrons is the large mean free path obtained for the electrons: in a container of 1.2 cm cathode radius, 0.08 cm anode radius and 5 cm height, electron mean free paths of 10^3 cm are reported¹.

The advancement on the construction and performance of operational amplifiers and the ease of construction of conventional ionization gauges have greatly contributed to diminish the concern for the orbitron as a vacuum gauge. On the other hand, its use as a vacuum pump has been established⁴ due to its lower power consumption and facility of its construction as compared with conventional magnetically confining devices for getter-ion pumps. As a pump, the performance of an orbitron improves the larger as the total space charge is increased and its distribution more uniformly distributed in space. This fact leads naturally to the study of the space charge distribution, both from the theoretical as well as experimental, points of view.

The earliest theoretical description of the orbitron's electron density was given by Hooverman⁵ as a superposition of noninteracting charge particle orbits in a logarithmic potential. In his description, it was assumed that the electrons moved in plane orbits, perpendicular to the axis of the orbitron, which slowly drifted in the axial direction. Under these assumptions, one is able to conclude, after investigating the geometry of the orbits, and assuming a sharp distribution in angu-

lar momentum, that the radial distribution of the electronic charge has two maxima corresponding roughly to the apogees and perigees of the plane orbits. This has been the major conclusion of Feaks et al⁶. Continuing in a somewhat similar reasoning, Deichelbohrer⁷ has discussed the effect on the charge density of different velocity distributions after the electrons leave the injector region. He showed that the electronic distribution is strongly dependent on assumptions made for the axial velocity as well as for the angular momentum distributions. In particular, the introduction of a spread in the axial velocity had the effect of lowering the electronic charge distribution near the cathode, and eventually eliminating the outer peak shown by the previous authors⁵.

Direct measurement of the electronic charge distribution is a difficult task, and so far has not been reported. Cybulska and Douglas⁸ have gotten evidences for the electronic charge distribution by measuring the energy spectrum of positive ions that reach the cathode, for low pressures, and small electronic total charge.

Let us call, $f(\vec{r}, \vec{p})$, the single particle distribution function in phase space, and let us suppose n_0 to be the density of neutral gas inside the orbitron. The yield, $dI/d\Omega$, of ions per unit volume, and time, can be written as

$$\frac{dI}{d\Omega} = eNn_0 \int d^3p \sigma v f(\vec{r}, \vec{p}), \quad (1.1)$$

where v is the speed of the electron and σ the ionization cross section for the neutral gas under consideration. We are assuming the gas atoms to have negligible speed as compared with the electron speed, v . Defining

$$\langle \sigma v \rangle = \int d^3p v \sigma f(\vec{r}, \vec{p}) / \int d^3p f(\vec{r}, \vec{p}), \quad (1.2)$$

and

$$n(\mathbf{r}') = -eN \int d^3p f(\vec{r}, \vec{p}), \quad (1.3)$$

where $n(\vec{r})$ is the electron space charge distribution, we have:

$$\frac{dI}{d\Omega} = -n_0 n(\vec{r}) \langle \sigma v \rangle . \quad (1.4)$$

Fig. 1 shows schematically the arrangement of the different parts of an orbitron. Cybulska's measurement of the ion currents were restricted to the region of the orbitron which is distant from the filament to diminish the effect due to the collection of primary electrons. In the central zone, we may assume the electrostatic field to have cylindrical symmetry, and if we further assume the ions to be produced with negligible kinetic energy, the energy of the ion hitting the cathode can be equated to the electrostatic potential energy acquired by the ion at the moment of its ionization. Therefore, the ions hitting the cathode, with energy between E and $E + dE$, come from the volume $d\Omega = 2\pi r l dr$ of the cylindrical shell of radius r , length l , of the central zone, where the potential $V(r)$ satisfies $eV(r) = E$. We have, therefore,

$$\frac{dI}{dE} = \frac{dI}{d\Omega} \left(\frac{2\pi r l}{e} \right) \frac{dr}{dV} . \quad (1.5)$$

Using Eq. (1.4), one obtains:

$$n(\vec{r}) = e (2\pi r l n_0 \langle \sigma v \rangle)^{-1} \frac{dI}{dE} \cdot \frac{dV}{dr} . \quad (1.6)$$

One sees from Eq. (1.6) that the measurement of dI/dE is directly related to $n(\vec{r})$. The potential $V(r)$ may be considered logarithmic in the limit of very low electronic charge in the interior of the orbitron, and therefore known and controlled by the experimental setup. On the other hand, $\langle \sigma v \rangle$ is sensitive on the model assumed for the electronic distribution in phase space. This fact makes it difficult the interpretation of Cybulska's measurement as the derived space charge is model dependent.

In this paper, we will discuss the theoretical background that led to the determination of $f(\vec{r}, \vec{p})$, and we consider one model for the explicit calculation of $f(\vec{r}, \vec{p})$ which differs substantially from the previous

considerations of Hooverman, Feaks and Deichelbohrer. This model is applied to the interpretation of Cybulska's experiment.

2. THEORETICAL CONSIDERATIONS

Let us consider N electrons interacting with an external potential $V_{\text{ext}}(r)$, and among themselves by their Coulomb interactions. The N -particle Hamiltonian can be written as

$$H = \sum_{i=1}^N \left\{ \frac{p_i^2}{2m} - eV_{\text{ext}}(r_i) \right\} + \frac{1}{2} \sum_{i,j=1}^N \frac{e^2}{r_{ij}}, \quad (2.1)$$

where $r_{ij} = |\vec{r}_i - \vec{r}_j|$.

The evolution in time of the N -particle system can be described by the distribution function $f_N(\vec{p}_1, \dots, \vec{p}_N, \vec{r}_1, \dots, \vec{r}_N, t)$ which satisfies Liouville's equation⁹

$$\frac{\partial f_N}{\partial t} = \sum_{i=1}^N \left(\frac{\partial H}{\partial \vec{r}_i} \cdot \frac{\partial f_N}{\partial \vec{p}_i} - \frac{\partial H}{\partial \vec{p}_i} \cdot \frac{\partial f_N}{\partial \vec{r}_i} \right). \quad (2.2)$$

The one- and two-particle distribution functions are defined as:

$$\begin{aligned} f_1(\vec{r}_1, \vec{p}_1, t) &= \int d^3r_2 \dots d^3r_N d^3p_2 \dots d^3p_N f_N, \\ f_2(\vec{r}_1, \vec{p}_1, \vec{r}_2, \vec{p}_2, t) &= \int d^3r_3 \dots d^3r_N d^3p_3 \dots d^3p_N f_N. \end{aligned} \quad (2.3)$$

Taking into consideration the fact that H involves only one- and two-particle interactions, and f_N is symmetric with respect to exchange of particles, one easily obtains

$$\begin{aligned} \frac{\partial f_1}{\partial t} + \frac{\vec{p}}{m} \cdot \frac{\partial}{\partial \vec{r}} f_1 - e \frac{\partial}{\partial \vec{r}} V_{\text{ext}}(\vec{r}) \cdot \frac{\partial f_1}{\partial \vec{p}} \\ - (N-1)e \int d^3r' d^3p' \frac{\partial}{\partial \vec{r}} \left(\frac{1}{|\vec{r}-\vec{r}'|} \right) \frac{\partial}{\partial \vec{p}} f_2(\vec{r}, \vec{p}, \vec{r}', \vec{p}', t) = 0. \end{aligned} \quad (2.4)$$

We now make the independent particle approximation, writing

$$f_2(\vec{r}, \vec{p}, \vec{r}', \vec{p}', t) = f_1(\vec{r}, \vec{p}, t) f_1(\vec{r}', \vec{p}', t), \quad (2.5)$$

from where, we obtain, substituting Eq. (2.5) into Eq. (2.4):

$$\frac{\partial f_1}{\partial t} + \frac{\vec{p}}{m} \cdot \frac{\partial f_1}{\partial \vec{r}} - e \frac{\partial V}{\partial \vec{r}} \cdot \frac{\partial f_1}{\partial \vec{p}} = 0, \quad (2.6)$$

where

$$V(\vec{r}, t) = V_{\text{ext}}(\vec{r}) + \int d^3 r' \frac{1}{|\vec{r} - \vec{r}'|} n(\vec{r}', t), \quad (2.7)$$

with

$$n(\vec{r}, t) = -e(N-1) \int d^3 p f_1(\vec{r}, \vec{p}, t). \quad (2.8)$$

We observe that $n(\vec{r}, t)$ is the electronic charge density, and $V(\vec{r}, t)$ the self-consistent electric potential, that is, the external electrostatic field $V_{\text{ext}}(\vec{r})$ together with the field produced by all the other electrons on the electron under consideration. Eq. (2.6) is a particular case of Vlasov's equation for plasmas¹⁰.

Let us define the single particle Hamiltonian by

$$h(\vec{r}, \vec{p}, t) = \frac{p^2}{2m} - eV(\vec{r}, t). \quad (2.9)$$

Then, Eq. (2.6) can be written as

$$\frac{\partial f_1}{\partial t} + \frac{\partial h}{\partial \vec{p}} \cdot \frac{\partial f_1}{\partial \vec{r}} - \frac{\partial h}{\partial \vec{r}} \cdot \frac{\partial f_1}{\partial \vec{p}} = 0, \quad (2.10)$$

which is Liouville's equation in the single particle phase space

We will now discuss the possible solutions, for Eq.(2.10), which describes the orbitron's space charge. Let us begin observing that the dependence of $V(\vec{x}, \vec{t})$, on $f_1(\vec{x}, \vec{p}, t)$, given by Eq.(2.8), makes Vlasov's equation nonlinear. If q_0 is the charge per unit of length in the anode, for maintaining the electrostatic field in the absence of space charge, and q the space charge per unit of length of the orbitron, the dimensionless parameter,

$$\lambda = q/q_0 \quad (2.11)$$

is a good measure for the influence of the space charge on $V(x)$. The charge q_0 is given by

$$q_0 = 2\pi V_0 / \ln(b/a), \quad (2.12)$$

where V_0 is the anode potential, and b and a the cathode and anode radii, respectively. Assuming Cybulska's orbitron parameters: $V_0 = 800V$, $b = 4.5 \text{ cm}$ and $a = 0.08 \text{ cm}$, and expressing q_0 in units of the electron charge we get

$$q_0 = 4 \times 10^8 e .$$

Cybulska's reported value for λ is $\lambda = 0.08$, which gives

$$q = 3 \times 10^7 e \quad (2.13)$$

for the space charge per unit of length.

the low value for λ , in Cybulska's experiment, justifies the linear approximation for Vlasov's equation, what greatly simplifies the calculations.

Let us now observe that any function of the Hamiltonian $h(\vec{x}, \vec{p})$ is a stationary solution of Eq.(2.10), and different authors have put forward models considering different choices for this function.

Let us restrict our discussion to stationary solutions, i.e., $V(r, t) \equiv V(r)$, and to the central zone of the orbitron, where we may assume cylindrical symmetry for $V(r)$. We write:

$$h = \frac{1}{2m} \left(p_r^2 + \frac{L^2}{r^2} + p_z^2 \right) - eV(r) \quad , \quad (2.14)$$

where p_r is the radial momentum, p_z the axial momentum, and L the axial component of the angular momentum. The coordinate r measures the distance to the axis of symmetry. Besides the energy, both L and p_z are constants of motion, and therefore a choice for the solution of Eq. (2.10) is

$$g(E_0, L_0, p_0, r, p_r, L, p_z) = K \delta(E_0 - h) \delta(L_0 - L) \delta(p_0 - p_z) \quad , \quad (2.15)$$

where K is a normalization constant.

Due to the linear character of Eq. (2.10), a general solution can be constructed as a superposition of solutions of the form given by Eq. (2.15), and we have

$$f(r, p_r, L, p_z) = \int dE_0 dL_0 dp_0 \rho(E_0, L_0, p_0) g \quad , \quad (2.16)$$

where $\rho(E_0, L_0, p_0)$ is an arbitrary function subject only to the normalization condition,

$$\int dE_0 dL_0 dp_0 \rho = 1 \quad .$$

It is quite clear, from the structure of Eq. (2.16), that $\rho(E_0, L_0, p_0)$ sets the boundary conditions for the solution of Eq. (2.10), and all the previous theoretical works done on the orbitron's space charge can be understood as alternative choices for $\rho(E_0, L_0, p_0)$. In this sense, we will discuss particularly Deichelbohrer's paper, not only for being the most recent but also because he summarizes, to a great extent, the previous results.

Deichelbohrer relates the choice of $\rho(E_0, L_0, p_0)$ to the injection mechanism as he neglects any consideration for the electron - electron scattering inside the orbitron. Thus, he concludes that all the electrons have the same energy, \bar{E} , given by the position and bias of the filament. Hence,

$$\rho(E_0, L_0, p_0) = \delta(\bar{E} - E) \rho'(L_0, p_0) . \quad (2.17)$$

Next he considers the upper and lower limits for L_0 and p_0 . For the upper limit of L_0 , he takes the value which corresponds to the circular orbit which passes through the filament position and the lower limit to the orbit which grazes the anode surface. The momentum p_0 varies from zero to the upper allowed value corresponding to that orbit which leaves the injector region in a straight axial movement. Apart from these boundaries dictated by the conditions set by the filament, the actual shape of $\rho'(L_0, p_0)$ in Eq. (2.17) is not determined. To proceed, Deichelbohrer makes a further simplification by factoring $\rho'(L_0, p_0)$:

$$\rho(E_0, L_0, p_0) = \delta(\bar{E} - E_0) \rho_1(L_0) \rho_2(p_0) . \quad (2.18)$$

He assumed two shapes for each factor. For $\rho_1(L_0)$, he considered (i) a uniform distribution, and (ii) $\sin^2(\pi L_0/L_m)$ where L_m is the upper limit for L_0 . For $\rho_2(p_0)$, he assumed (i) a sharp distribution at $p_0 = 0$, and (ii) a uniform one. These assumptions combine in four possible choices for $\rho(E_0, L_0, p_0)$, and Fig.2 exhibits the results obtained. One observes that the charge distribution is strongly dependent on the shape assumed for $\rho_1(L_0)$ and $\rho_2(p_0)$ and we are therefore led to wonder if a more general principle can be invoked to restrict the possible choices of distributions. This was the approach adopted by the works of oliveira** , Pato¹² and Rogerio¹³ which we will consider from now on. The essential point we would like to stress is the well known result of statistical mechanics that if one rigorously carries out the hypothesis of the absence of interaction among the electrons, any initial distribution generates a stable distribution for the gas. As

soon as one considers the interparticle interaction, this is no longer true, and the distribution approaches a unique stable distribution, characterized by the maximum of entropy, in a time t characteristic of the relaxation of the initial distribution of the gas. If the mean lifetime of the electron, inside the orbitron were infinite, there would be no question that the statistical equilibrium would be reached. Actually, the electrons remain, inside the orbitron, only during a mean time τ , and the question we pose is whether τ is much smaller or much larger than t . Hooverman, Feaks and Deichelbohrer assume $\tau \ll t$, and conclude that the initial distribution, dictated by the injection conditions at the filament, prevails during the whole life of the electron in the orbitron. Oliveira, Pato and Rogerio made the opposite assumption, i.e., that $t \ll \tau$, and therefore the distribution is dictated by the statistical equilibrium reached by the electrons. It is quite clear that the two choices are extreme ones, and the actual situation is expected to be in an intermediate one. Once the statistical equilibrium is assumed, we may conclude that the energy distribution is canonical, and we set

$$\rho(E_0, L_0, p_0) \cong \exp(-\beta E_0),$$

which gives, from Eq.(2.16),

$$f_1(x, p_r, L, p_z) \cong \exp(-\beta h(x, p_r, L, p_z)). \quad (2.19)$$

Due to the fact that the electrons participating of the space charge are those which do not touch the inner walls of the orbitron, we assume that Eq.(2.19) is valid only in a region R of the phase space which excludes possible trajectories that touch the walls. Under these assumptions, the charge distribution is given by

$$n(r) = A \int_{\Omega} dp_r \frac{dL}{r} dp_z \exp(-\beta h), \quad (2.20)$$

and we observe that now we have only one undetermined parameter, β , (playing the role of the inverse temperature of the electron gas), besides the normalization constant A.

3. THE CHARGE DISTRIBUTION

We will determine, in this Section, the domain of integration for Eq. (2.2) under the assumption that electrons which collide with the anode or cathode of the orbitron are extracted from the space charge. As we will be only interested in the determination of $n(\vec{r})$ for the central region of the orbitron, we will assume as before that $V(r)$ and $n(\vec{r})$ have cylindrical symmetry. Due to electron-electron collisions, electrons at a position \vec{r} may acquire enough radial momentum to be able to collide with the anode or cathode. We assume that whenever an electron is energetically able to reach the walls of the orbitron, we exclude it from the distribution. This is justified on the assumption that the mean free path between collisions is larger than the radial dimensions of the orbitron. This condition sets up limits for p_r , and one may verify that we have to impose the restriction

$$\frac{p_r^2}{2m} < \frac{L^2}{2ma^2} - eV_0 - \left(\frac{L^2}{2mr^2} - eV(r) \right) \quad (3.1)$$

for the electrons not to hit the anode, of radius a , and potential V . The similar condition for not hitting the cathode is

$$\frac{p_r^2}{2m} < \frac{L^2}{2mb^2} - \left(\frac{L^2}{2mr^2} - eV(r) \right), \quad (3.2)$$

where b is the radius of the cathode assumed to be grounded.

We rewrite Eqs.(3.1) and (3.2) in the following forms that exhibit better the geometrical restrictions on the (p_r, L) space:

$$\frac{L^2}{L_1^2} - \frac{p_r^2}{p_1^2} > 1,$$

and

$$\frac{L^2}{L_2^2} + \frac{p_r^2}{p_2^2} < 1, \quad (3.3)$$

where

$$L_1^2 = \frac{2me(V_0 - V)a^2r^2}{r^2 - a^2},$$

$$p_1^2 = 2me(V_0 - V), \quad (3.4)$$

$$L_2^2 = \frac{2meVb^2r^2}{b^2 - r^2},$$

and

$$p_2^2 = 2meV.$$

Fig.3 shows the regions of allowed values, for L and p_r , indicated by the shaded areas. Defining L_3 as indicated by Fig.3, we can set the limits of integration for L and p_r :

(i) for $L_1 < |L| < L_3$:

$$|p_r| < p_1 \left(\frac{L^2}{L_1^2} - 1 \right)^{1/2} \equiv \omega_1; \quad (3.5)$$

(ii) for $L_3 < |L| < L_2$:

$$|p_r| < p_2 \left(1 - \frac{L^2}{L_2^2} \right)^{1/2} \equiv \omega_2; \quad (3.6)$$

and L , is given by the following equation:

$$p_2 \left(1 - \frac{L_3^2}{L_2^2} \right)^{1/2} = p_1 \left(\frac{L_3^2}{L_1^2} - 1 \right)^{1/2}$$

which gives

$$L_3^2 = \frac{2me V_0 a^2 b^2}{b^2 - a^2} \quad (3.7)$$

In principle, we should also have set up limits for the axial component of the momentum. As we are interested only in the central region of the orbitron, one may imagine the orbitron to be infinitely long, and neglect any such limitations for p_z , assuming the limits for p_z to be $+\infty$ and $-\infty$. Finally, we arrive at the explicit expression for $n(r)$:

$$\begin{aligned} n(r) = & \frac{A}{r} \int_{L_1}^{L_3} dL \int_0^{\omega_1} dp_r \int_0^\infty dp_z \exp(-\beta h) \\ & + \frac{A}{r} \int_{L_3}^{L_2} dL \int_0^{\omega_2} dp_r \int_0^\infty dp_z \exp(-\beta h). \end{aligned} \quad (3.8)$$

Let us observe that for $r=a$, i.e., at the anode, $\omega_1=0$ and the integration over p_r vanishes in the first term of the right hand side of Eq. (3.8). The second term also vanishes at the anode due to the fact that $L_1 = L_3$ and $\omega_2=0$, for $r=a$. Hence, $n(r)$ is zero at the anode. In an analogous way, one can show that $n(r)$ is also zero at the cathode, which shows that $n(r)$, given by Eq. (3.8), is zero at the inner surface of the orbitron.

Making explicit use of the form of h , exhibited in Eq.(2.9), and of the normalization constant, we finally obtain:

$$2\pi r n(r) = eNA \exp(-\beta V) g(r, V, \beta), \quad (3.9)$$

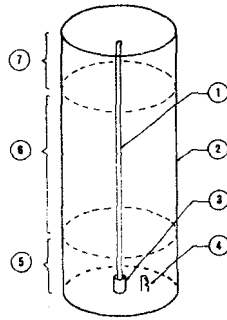


Fig. 1 - A schematic drawing of an orbitron; 1 - is the anode rod ; 2 - the cathode cylinder; 3 - the reflector tube; 4 - the filament . The orbitron can be thought as divided in three zones; 5 - the filament zone; 6 - the central zone, and 7 - the far zone.

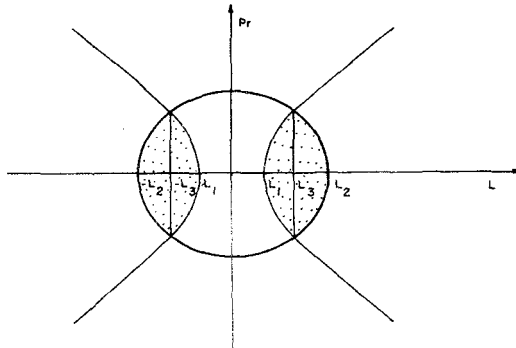


Fig. 3 - The allowed region in the (p_r, L) plane of the phase space, at a given position z , indicated by the shaded areas. The values of L_1 , L_2 and L_3 are given in the text by the Eqs.(3.3), (3.4) and (3.7), respectively.

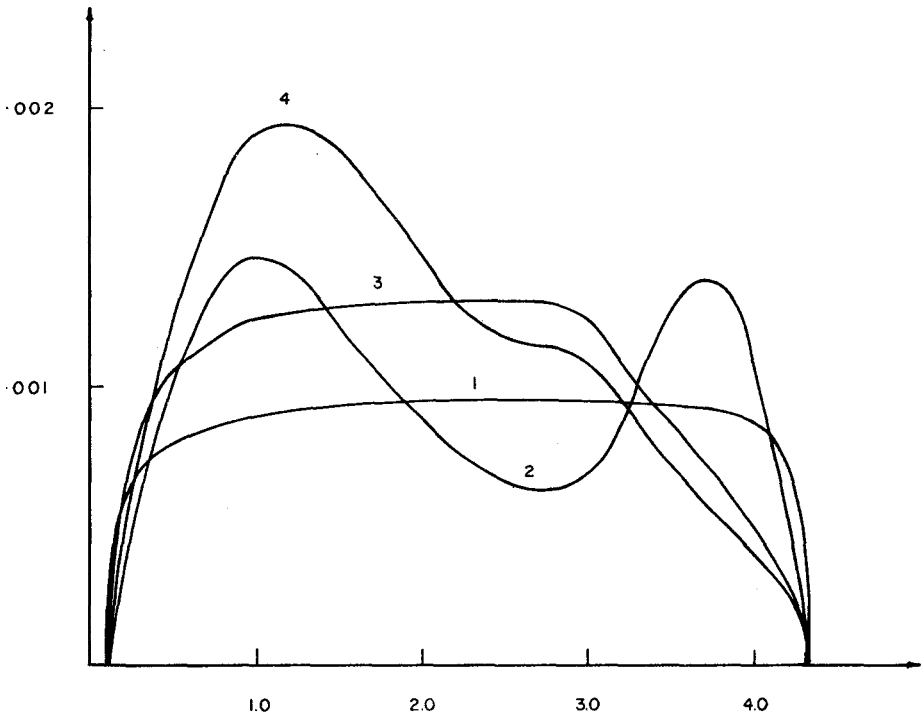


Fig. 2 - The four radial electron distributions obtained from the four models described by Deichelbohrer⁷. Curve 1 corresponds to a uniform distribution in angular momentum, and a sharp distribution at zero axial momentum. Curve 2 corresponds to the $\sin^2(\pi L/L_m)$ distribution in angular momentum, and the same as curve 1 for the axial momentum. Curve 3 corresponds to a uniform distribution for the axial and angular momenta. Curve 4 corresponds to the $\sin^2(\pi L/L_m)$ distribution for angular momentum, and uniform distribution in axial momentum.

where

$$A^{-1} = \int_a^b dr \exp(-\beta V) g(r, V, \beta),$$

and

$$g(r, V, \beta) = \int_{L_1}^{L_3} dL \exp\left[-\frac{\beta L^2}{2mr^2}\right] \operatorname{erf}(\omega_1 \beta^{1/2}) \\ + \int_{L_3}^{L_2} dL \exp\left[-\frac{\beta L^2}{2mr^2}\right] \operatorname{erf}(\omega_2 \beta^{1/2}). \quad (3.10)$$

Equations (3.9) and (3.10) give $n(r)$ explicitly as a function of $V(r)$ and the parameter β , which can be solved by iteration with Eq.(2.7), resulting in the selfconsistent charge distribution. Due to the cylindrical symmetry, Eq.(2.7) can be put in a simpler form by making use of Gauss' theorem:

$$V(r) = V_0 \ln(r/r_0) / \ln(a/r_0) + 4\pi \int_0^r \frac{dr'}{r'} \int_0^{r'} r'' n(r'') dr'', \quad (3.11)$$

with the parameter r , fixed by the condition $V(b) = 0$.

4. THE RESULTS

Let us introduce the dimensionless coordinate $x = r/b$, where b is the cathode radius, and let us call

$$x_0 = a/b, \quad (4.1)$$

and

$$\alpha = eV_0/kT, \quad (4.2)$$

where a is the anode radius, V_0 the anode potential, and we introduced

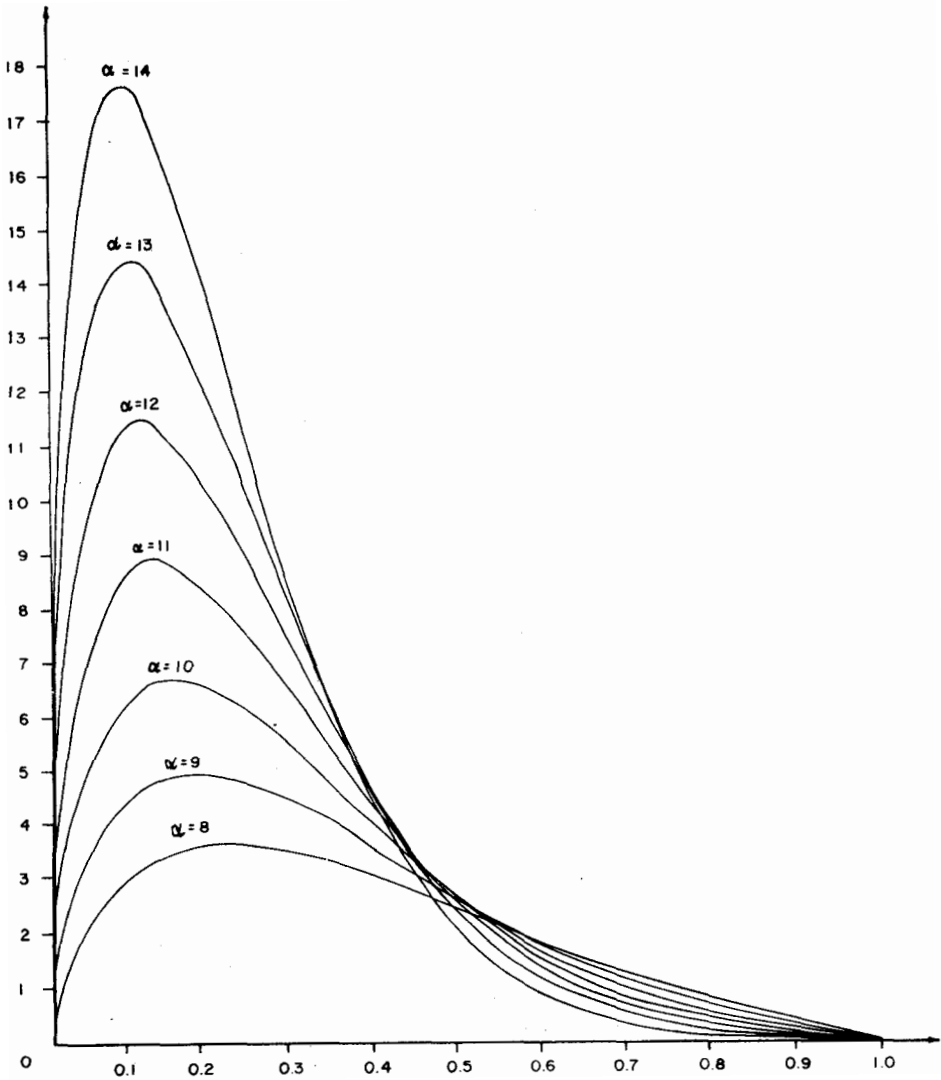


Fig. 4 - The function $\eta(x)$, defined by Eq.(4.3), versus the function $y(x)$, given by Eq.(4.5), for different values of the parameter α . The value of x_0 is 0.0133.

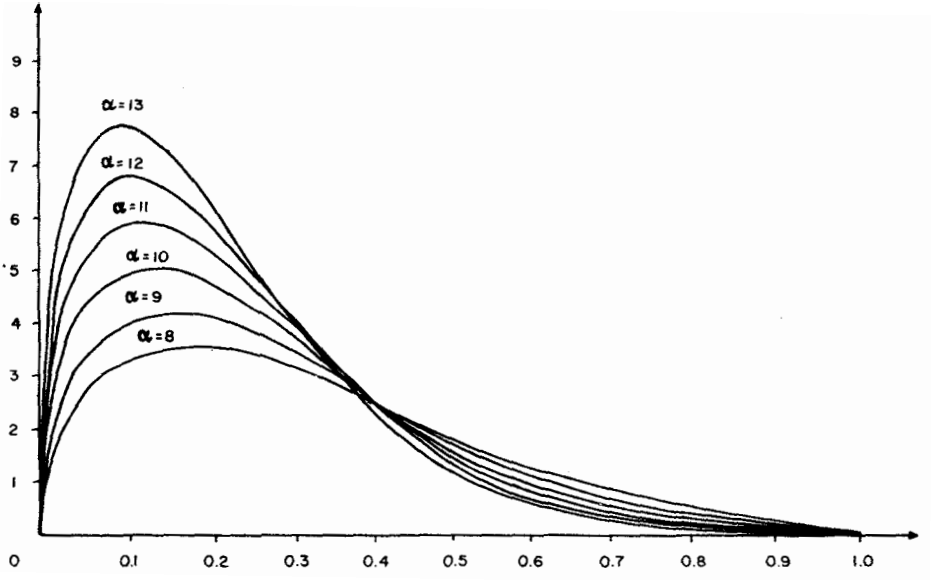


Fig. 5 - The same as in Fig. 4 except that $x_0 = 0.10$.

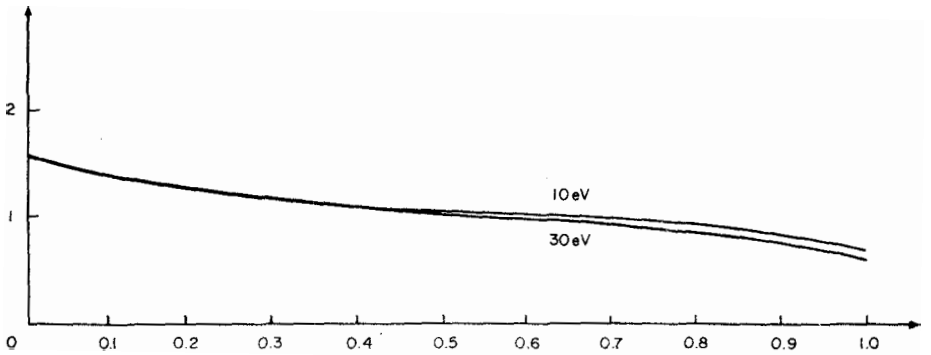


Fig. 6 - The function $\langle \nu \sigma \rangle$ plotted as function of $y(x)$, for two values of the threshold energy for ionization: 10eV and 30eV as indicated.

$$\beta^{-1} = kT ,$$

in conformity with the usual practice in statistical mechanics, where k is the Boltzmann constant, and T the temperature of the electron gas. With these definitions, one can easily show that $2\pi r n(r)$, given by Eq. (3.9), can be written in terms of the dimensionless function $\eta(x)$, that is:

$$2\pi r n(r) = \frac{q}{L} \eta(x) , \quad (4.3)$$

where q is the previously defined total space charge per unit of length, and we are normalizing $\eta(x)$ such that

$$\int_{x_0}^1 \eta(x) dx = 1 . \quad (4.4)$$

We further define

$$y(x) = 1 - (\ln x / \ln x_0) , \quad (4.5)$$

and we observe that $y(x)=0$, at the anode, and unit at the cathode, positions. As we are interested in the comparison of our results with Cybulska's data, we will neglect the space charge contribution to the external potential. In this case, the function $\eta(x)$ depends only on the two dimensionless parameters a and x_0 . Fig. 4 shows $\eta(x)$ for different values of a , varying by unit from 8 to 14, with $x_0 = 0.0133$ corresponding to the geometry used in Cybulska's orbitron. Fig. 5, again, shows $\eta(x)$ for different values of α as indicated, but with $x_0 = 0.1$. In both figures, the abscissas are $y(x)$. We observe that, as already proven, $\eta(x)$ vanishes at the cathode ($y=1$) and anode ($y=0$). In all cases, the distributions present only one peak quite close to the anode. The larger the value of a , i.e., the smaller the electron temperature for a fixed voltage V_0 , the sharper is the peak. The effect of increasing the anode radius is to broaden the peak of the distribution.

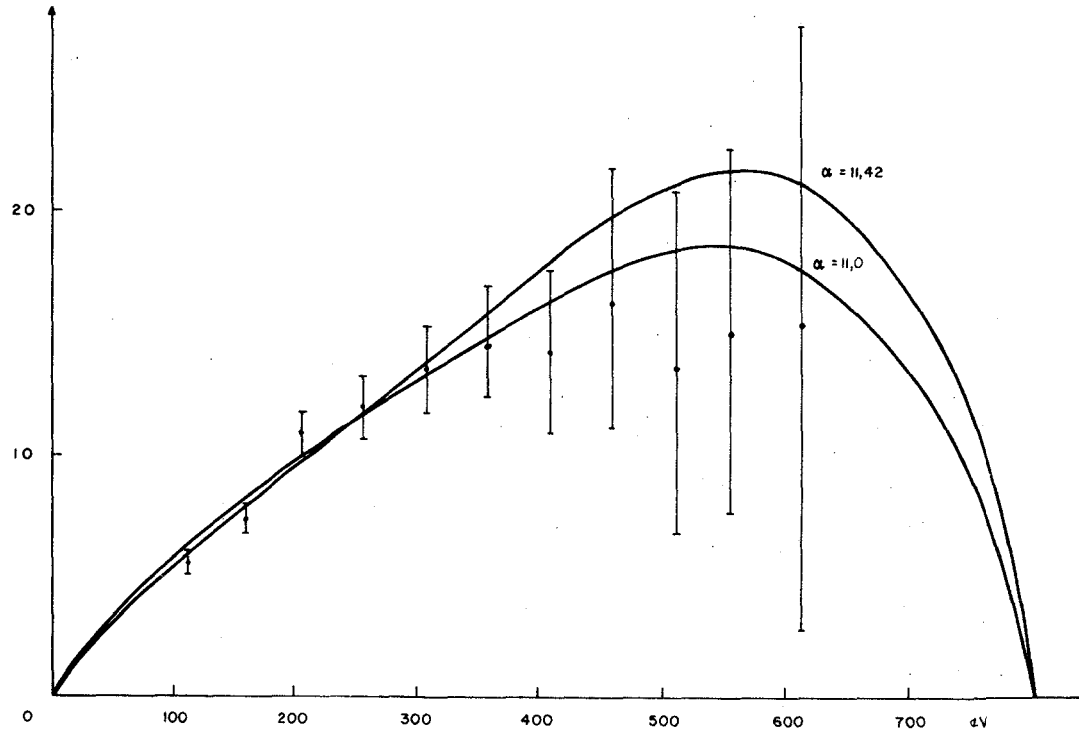


Fig.7 - The experimental points obtained by Cybulska⁸ for the positive ion energy-density spectrum. The horizontal axis is the energy eV in units. The two solid curves correspond to the predictions of Pato's model for two values of the parameter α , as indicated.

The average $\langle v \sigma \rangle$ can be calculated by numerical integration. We approximated the empirical data on the ionization cross section, $\sigma(E)$, by a step function and considered two extreme cases, where the threshold energy in $\sigma(E)$ is 10eV and 30eV. Fig.6 exhibits our results. We observe that $\langle v \sigma \rangle$ is a slowly varying function of position, and depends weakly on the threshold energy. These results give us confidence to interpret Cybulska's data on the ion energy spectrum. Figure 7 shows the experimental data and our theoretical prediction for two values of α . We assumed the threshold energy to be 20eV, and x_0 equal to 0.0133 corresponding to Cybulska's orbitron geometry. We should observe the rather good agreement with the experimental data, which suggest that our basic assumption, for the attainment of statistical equilibrium of the electron gas, is a reasonable one. Using our result for $\langle v \sigma \rangle$, we can reduce the ion energy-density spectrum into $\eta(x)$ data. This is shown in Fig. 8, where the horizontal axis is, again, $y(x)$. We should also observe that $n(x)$, which is proportional to $\eta(x)$, has a maximum at approximately $y=0.15$ or $x=0.12\text{cm}$. Our prediction for $n(x)$ is, therefore, a distribution with a sharp peak very near the anode.

5. CONCLUSIONS

The models advanced, for the determination of the charge distribution in orbitrons, can be divided into two classes: (i) those which assume that the initial conditions, dictated by the filament environment, prevail during the whole lifetime of the electrons, and (ii) those which assume that the electron-electron collisions are frequent enough to establish a statistical equilibrium. These two assumptions can be understood as extreme cases, and the basic question is which of these conditions more closely represents the real condition in the orbitron. Cybulska and Douglas⁸ have made comparisons of their measurements with one of the four models calculated by Deichelbohrer, which belongs to the first class, and their findings were that Deichelbohrer's model⁷ does not predict accurately the experimental observations. We have in this paper proposed a model based on statistical equilibrium, and the comparison with the experimental data was very satisfactory, giving

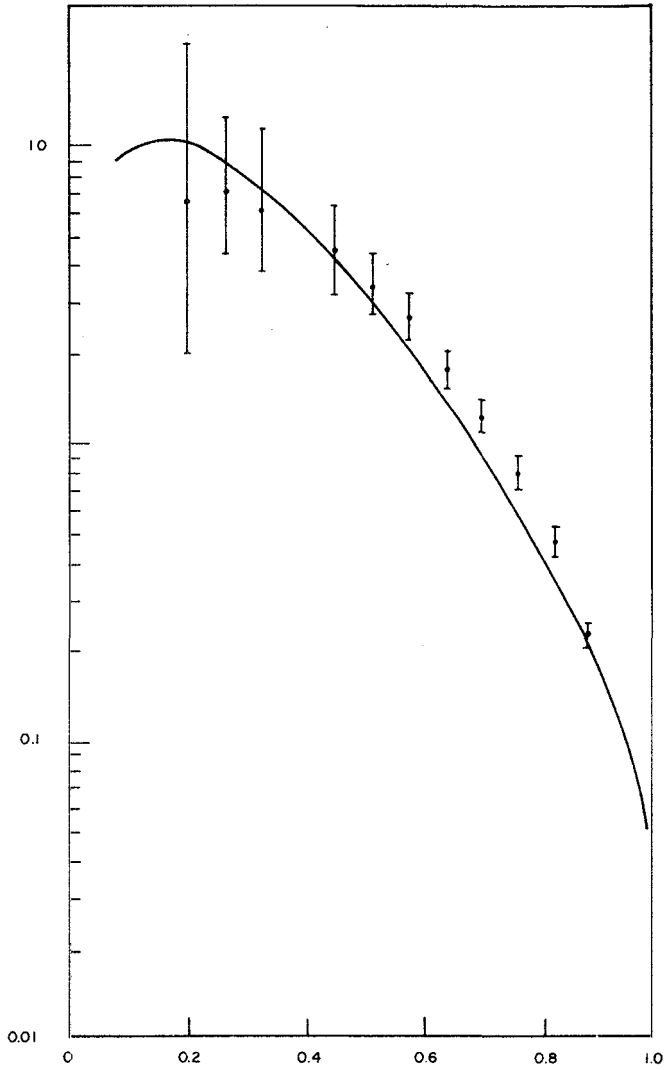


Fig. 8 - The electron density function $\eta(x)$, defined in Eq.(4.3), for $a = 11.42$ and $x_0 = 0.0133$, plotted against $y(x)$, adjusted to give the best fit to the positive ion energy-density spectrum measured by Cybulska. The vertical scale is logarithmic. Also, the experimental points are shown for the ion energy density spectrum reduced to $\eta(x)$ data.

credibility to the statistical assumption. A better check, on which class of models is closer to the prevailing situation inside the orbitron, would be the study of the positive ion energy density spectrum, for different positions and geometries of the filament. An insensitivity of the measurement, on these parameters, would verify that the initial conditions, at the filament, are not important. Hence, the electron-electron collisions would be important to erase the peculiarities of the initial conditions, at the filament, on the prevailing charge distribution. These measurements, unfortunately, have not been done so far. From the theoretical side, the study of the space charge effect, on the self-consistent potential, should be carried out, as the only study done so far is the one by oliveira¹³ but with simplified boundary conditions.

From our point of view, it is simple to understand why an upper limit to the number of electrons, in orbitrons, should exist. The predicted distribution is greatly confined to a small volume around the anode. With an increasing number of electrons, the space charge deforms the electrostatic potential, making it practically zero for distances even less than the filament distance to the anode. In a sense, the effect of increasing the number of electrons is to reduce the radial dimension of the orbitron. Under these conditions, the filament would be unable to inject more electrons into the electron cloud. This, of course, occurs intermitently. Once the filament is shielded, the space charge starts to diminish by losing electrons, through electron-electron collisions, and soon the filament is again able to inject more electrons into the cloud, repeating the cycle again. This intermitent regime is responsible for exciting acoustic waves in the electron gas, which are observed as electromagnetic oscillations associated with the high density regime. These oscillations have been observed by Troise and Douglas¹⁴.

The authors would like to thank Ewa Cybulska and Ross Douglas for making available their data prior to publication, and for many helpful discussions. One of us (L.C.G.) would like to thank Oscar Sala for the hospitality of the Pelletron Laboratory.

REFERENCES AND NOTES

1. R.G. Herb, T. Pauly and K. J. Fisher, Bull. Am. Phys. Soc. 8, 336 (1963).
2. W.B. Mourad, T. Pauly and R.G. Herb, Rev.Sci.Instr. 35, 661 (1964).
3. R.A. Douglas, J. Zabritski and R.G. Herb, Rev.Sci.Inst. 36, 1 (1965).
4. For example, the São Paulo Pelletron accelerating tube is pumped by orbitrons.
5. R.H. Hooverman, J. Appl. Phys. 34, 3505 (1963).
6. F. Feaks, E.C. Muly and F.J. Brock, *Extension of gauge calibration study in extreme high vacuum*, a NASA publication under contract NAS-W-1137.
7. P.R. Deichelbohrer, J. Vac. Sci. Technol., 10, 875 (1973).
8. E.W. Cybulska and R.A. Douglas, preprint, *The Radial Charge Distribution in an Orbitron*, Dep. de Física Nuclear. Universidade de São Paulo, São Paulo, SP.
9. We use $\partial/\partial\vec{x}$ to represent the gradient with respect to the three dimensional vector \vec{x} .
10. See, for example, R. Balescu, *Statistical Mechanics of Charged Particles*, Wiley-Interscience, New York, N.Y., 1963.
11. N. T. Oliveira, Thesis, Departamento de Física, Universidade de Brasília, Brasília, D.F., Brazil (1971).
12. M. P. Pato, Thesis, Departamento de Física, Universidade de Brasília, Brasília, D.F., Brazil (1971).
13. R.F. Rogerio, Thesis, Departamento de Física, Universidade de Brasília, Brasília, D.F., Brazil (1971).
14. S. J. Troise, Thesis, Departamento de Física, F.F.C.L. da U.S.P., São Paulo, SP, Brazil (1970).